

# ELEET- Formulating a Multi-Element, Inter-agency Error Budget for Robust Earth Entry of Returned Mars Samples\*

Alan M. Didion<sup>1</sup>, Alexander R. Tompkins<sup>2</sup>, Austin K. Nicholas<sup>3</sup>, and Marcus A. Lobbia<sup>4</sup>

*Jet Propulsion Laboratory, California Institute of Technology, Pasadena, CA, 91011, USA*

The operational segment of a potential Mars Sample Return campaign could end with final delivery of the Earth Entry System to the surface of Earth, punctuating an impressive international collaboration on multiple flight elements over many years. A comprehensive error budget approach is presented to characterize the high-dimensional technical challenge of this concept, including inputs from interdisciplinary stakeholders. Effects considered include interplanetary navigation, spacecraft attitude and maneuver control, and entry environment, culminating in figures of merit such as landing range accuracy. Broad tradespace exploration confirms some intuitions while challenging others, and a set of solutions are identified that are mutually agreeable to NASA and ESA.

## I. Nomenclature

$e$	=	eccentricity of the orbit
$\Delta t$	=	change in time
$F$	=	eccentric anomaly
$H$	=	hyperbolic anomaly
$M$	=	mean anomaly
$v$	=	true anomaly
$\mu$	=	Earth's gravitational parameter
$r$	=	orbital radius relative to Earth's center
$v$	=	orbital velocity relative to Earth's center
$f$	=	F function
$g$	=	G function
$p$	=	semi-latus rectum of the orbit
$n$	=	generic index; orbital mean motion
$N$	=	generic counter; number of Monte Carlo samples

\* © 2019 California Institute of Technology. Government sponsorship acknowledged.

<sup>1</sup> Systems & Mission Design Engineer, Project Systems Engineering, Mission Concept Systems Development

<sup>2</sup> Co-op Student, Project Systems Engineering, Internal Build Mission Project Systems Engineering

<sup>3</sup> Systems Engineer, Project Systems Engineering, External Build Mission Project Systems Engineering

<sup>4</sup> EDL Systems Engineer, Flight Systems Engineering, EDL Systems and Advanced Technologies

## II. Introduction

The operational segment of a potential Mars Sample Return (MSR) campaign would end with final delivery of the Earth Entry System (EES) to the surface of Earth, punctuating an impressive feat of international collaboration on multiple flight elements over many years [1] [2] [3]. The baseline concept of EES delivery itself represents a tightly orchestrated sequence of events with multiple figures of merit (FOM) and error contributors such as navigation accuracy, orbiter attitude control, and maneuver execution errors. These error contributors and FOMs are “owned” by multiple mission elements and organizations (e.g. the EES from NASA [4] and the ERO from ESA [5]), so management of these resources is key.

In order to examine the quantitative effects of the numerous inputs in this challenge, an agile and versatile tool was needed that could explore the broad tradespace at hand. The EES Landing Ellipse Error Tool (ELEET) was created with the ultimate goal of informing an activity to allocate error contributions to each of the contributors to ensure accurate and robust final delivery during the EES Delivery Phase (EDP) as evaluated based on various FOMs which are often at odds (e.g.: landed accuracy vs. the amount of time spent tracking and planning).

### A. EDP Scenario Description

The final leg of the Earth Return Orbiter (ERO) trajectory starts about 30 days before entry and is known as the EDP, wherein the ERO arrives at Earth after a Solar Electric Propulsion (SEP) cruise from Mars and delivers the EES to its final course to land, notionally in the Utah Test & Training Range (UTTR). Rather than targeting direct entry from heliocentric space, the ERO targets a fail-safe trajectory which would miss Earth at a specified altitude if control of the spacecraft were lost. Days before entry, once all necessary tests have been performed and approvals have been given, the ERO would perform an Earth Targeting Maneuver (ETM), followed by an optional Final Cleanup Maneuver (FCM), and release of the EES on its intercept course. After delivery to an intercept trajectory, the ERO would divert its course to avoid impacting Earth itself, via an Earth Avoidance Maneuver (EAM). The EAM would be designed specifically to avoid gravitational keyholes in Earth’s B-plane such that the ERO will not return to contaminate Earth within at least 100 years.

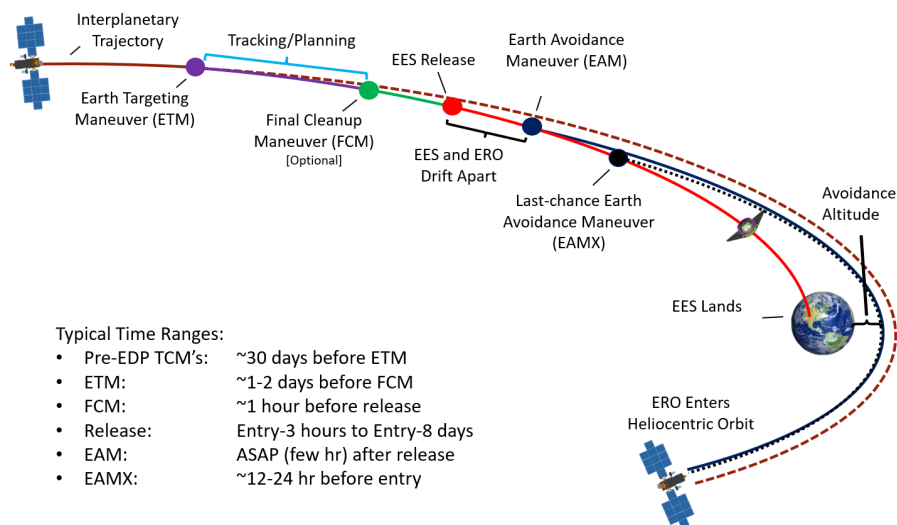


Figure 1. A cartoon of the EDP shows the relative timing/positioning of each of the trajectory segments leading up to EES delivery and Earth avoidance.

Below, each chronologically-ordered stage of the EDP is described in more detail:

- Transition from Interplanetary Cruise- The ERO arrives in the Earth system, its trajectory is subject to navigation errors, maintaining a fail-safe hyperbola which misses Earth by a given altitude. The magnitude of the miss altitude is a campaign FOM with regards to planetary protection and orbital debris avoidance.
- Earth System Cruise- The ERO cruises until the appointed time for ETM execution. The timing of ETM influences the final EES landing accuracy and is a risk-control FOM with regards to the total time available to execute the entire sequence, including margin.
- Earth Targeting Maneuver- An ETM is solved for by the ground and executed by the ERO, subject to stochastic maneuver execution and attitude control errors. The necessary stringency of these errors directly affects the implementation of the ERO systems.
- Tracking & Planning- After a variable period of tracking, navigation accuracy is improved as a function of both time and Earth-range. Time-on-intercept is a risk-control FOM which ultimately affects ERO robustness requirements.
- Final Cleanup Maneuver- If needed, an optional FCM can be planned and executed to clean up ETM errors and their effects on landing accuracy.
- EES Release- The EES is released from the ERO's hangar on the targeted trajectory, subject to various release mechanism and ERO attitude control errors. This has an effect of the final landing accuracy and the stringency of these errors directly affect the implementation of the EES re-lease mechanism.
- Earth Avoidance Maneuver- An EAM is executed to prevent ERO from impacting Earth and to target an appropriate flyby B-plane intercept to prevent the ERO from returning to Earth. The amount of time remaining to perform contingency maneuvers and the resulting  $\Delta V$  magnitude are FOMs.
- EES Entry- The EES enters Earth's atmosphere under the velocity and flight path angle conditions determined by the delivered trajectory. How extreme this entry environment is is a FOM of primary concern to EES implementation. These conditions also affect the final landing accuracy.
- EES Landing- Finally, the EES lands according to all of the effects imparted by the trajectory and atmospheric effects. The distribution of these landing states represents the primary accuracy FOM of the investigation.

After EES release, the scenario branches into an EES branch ("Ground Recovery Operations") and an ERO branch ("ERO Retirement"). ELEET covers the entirety of the EDP up through the delivery of the EES to the ground and the ERO to an Earth-miss trajectory. This paper describes the models that comprise ELEET, their sources, and how they come together in a MATLAB implementation to facilitate holistic trend and tradespace exploration. The primary FOMs are described from the perspective of each stakeholder, and trends and results are analyzed to find inflection points/minima/maxima in this high-dimensional tradespace to identify the optimal trajectories and sequences. This paper describes the ELEET model approach as applied to this problem and some select findings of the investigation.

### III. Methodology

During early discussions regarding this problem, it became clear that a readily customizable tool would be necessary. No existing framework was identified that could address this topic in the breadth and cadence desired, so ELEET was built as a piece of modular MATLAB software. [Section III](#) of this paper describes the software framework, underlying models, some data sources, and the definitions of output FOMs used in ELEET.

#### A. MATLAB Architecture

The software architecture of ELEET was designed from the beginning with vectorized computation and parallelization in mind to facilitate fast processing of large batches of input parameter sets. MATLAB was chosen as the ELEET environment primarily for its strengths in this regard, and for its availability and ease of quick adjustments throughout development. Within ELEET, data is passed as high-dimensional arrays and processed with linear algebra whenever possible. Multiple core functions are processed in parallel and outputs are compiled periodically to minimize data loss in the event of exceptions. A full tradespace run often takes overnight and so everything is designed to operate unattended and catch and track error messages and their causes. Not every input set yields a feasible solution, so the top-level routines are robust to unexpected outputs.

Final trajectories can be exported either one at a time or in batches as SPICE kernel (SPK) files for further analysis in various visualization tools or for communicating the design with other sub-teams and stakeholders via a standard format. Generally, ELEET outputs are analyzed for trends and inflection- or break-points to identify regions of the

tradespace of interest for detailed investigation in higher-fidelity tools. Often, each investigation with ELEET inspects a different set of FOMs vs. a specific set of inputs, so most analyses of outputs use tailored post-processing or plot formats. Some samples of interesting trends discovered by ELEET will be discussed in [section IV](#) of this paper.

## B. Models and Data Sources

### 1. Orbit Propagation

The core propagation functions of ELEET use the analytical F and G functions to propagate forward in time or to a specific radius, as described by Vallado [6]. This method sacrifices perturbations from n-body and aspherical gravity but allows ELEET to skip intermediate steps and propagate directly to the next point of interest very quickly and enable the software to execute tens of thousands of individual trajectory arcs in less than a second on a personal workstation. Because ELEET is fundamentally a tool for examining the effects of error distributions rather than scalar effects, it is justified to neglect such forces that would be well understood and biased out in the nominal trajectory aimpoint a priori.

The specific formulations of the F and G method used in ELEET are detailed below in [Equations 1-5](#), which form separate “propagate to time” and “propagate to radius” functions. The time-based form is used more often, with the radius-based form required for propagation to points of atmospheric interface/landing. The formulation for propagating through time from time zero to a future (past, if negative)  $\Delta t$ , in seconds, is shown in [Equations 1 and 2](#).

$$f = 1 - \frac{r_1}{p} * (1 - \cos(v_1 - v_0)); \quad g = r_0 * r_1 * \frac{\sin(v_1 - v_0)}{\sqrt{\mu * p}}$$

$$f = \sqrt{\frac{\mu}{p}} * \tan\left(\frac{v_1 - v_0}{2}\right) * \left(\frac{1 - \cos(v_1 - v_0)}{p} - \frac{1}{r_1} - \frac{1}{r_0}\right); \quad g = 1 - \frac{r_0}{p} * (1 - \cos(v_1 - v_0)) \quad (1)$$

$$\begin{bmatrix} r_1 \\ v_1 \end{bmatrix} = \begin{bmatrix} f & g \\ f & g \end{bmatrix} * \begin{bmatrix} r_0 \\ v_0 \end{bmatrix}$$

where,

$$H_0 = 2 * \tanh^{-1}\left(\frac{\tan\left(\frac{v_0}{2}\right)}{\sqrt{\frac{e+1}{e-1}}}\right); \quad M_0 = e * \sinh(H_0) - H_0; \quad M_1 = M_0 + n * \Delta t$$

$$H_1 = H_0 - \frac{M_1 - e * \sinh(H_1) - H_1}{1 - e * \cosh(H_1)}; \quad v_1 = 2 * \tan^{-1}\left(\frac{e+1}{e-1} * \tanh\left(\frac{H_1}{2}\right)\right) \quad (2)$$

$$r_1 = \frac{p}{1 + e * \cos(v_1)}$$

and,

$$r_n = \|r_n\|; \quad v_n = \|v_n\|; \quad p = a * (1 - e^2); \quad n = \sqrt{\frac{\mu}{-a^3}} \quad (3)$$

Alternatively, when propagating to a given radial position, Equation 1 and 3 are still used, but  $r_1$  is given and  $v_1$  is found via Equation 4 and the time of flight between the initial and final positions can be calculated using Equation 5.

$$v_1 = \frac{v_0}{|v_0|} * \cos^{-1}\left(\frac{p}{e * (r_1 - 1)}\right) \quad (4)$$

$$F_n = \cosh^{-1} \left( \frac{e + \cos(v_n)}{1 + e * \cos(v_n)} \right) \quad (5)$$

$$\Delta t = \sqrt{-\frac{a^3}{\mu} * ((e * \sinh(F_1) - F_1) - (e * \sinh(F_0) - F_0))}$$

Both methods are useful for propagating forward or backward quickly using a closed-form analytical and reversible solution. Note that if the goal radius is less than the perigee of the trajectory, the “propagate to radius” method will fail. ELEET includes error catches to throw out cases in which initial guesses or dispersed states miss the target altitude and records these as “rogue cases”. The count of rogue cases can be used as a measure of feasibility and chaotic behavior of a given parametric input. This enables the user to identify asymptotes and singularities in addition to regions of extreme sensitivity to inputs.

Further, implementation of these closed-form equations in MATLAB allows us to execute this method on arrays of inputs at once. For example, the function “propagate to time” ingests inputs of body/physical constants, an array of propagation times of size Nx1, and either a single initial state or a separate initial state for each of the N cases, and outputs the corresponding state for each case. This serves a primary purpose of processing a full Monte Carlo data set simultaneously, but can also be used to fill in a trajectory plot, solving for the state at each of time value, for example.

The astrodynamics output of ELEET was validated against simulations in AGI’s Systems Tool Kit (STK) and NASA’s General Mission Analysis Tool (GMAT) with two-body gravitation. Higher-order gravity or additional body terms were shown to produce scalar changes on the final trajectory, but have little effect on the shape and size of the distribution about the nominal over the range of trajectories in ELEET’s scope. Since ELEET is aimed at modeling the error distribution of the trajectory, the scalar differences in the nominal trajectory produced by e.g. solar gravity and solar radiation pressure (SRP) would be accounted for in the nominal design and neglecting them for error budget analyses is valid. Sources which do have significant uncertainty on their effect, such as SRP, get their own error models which add into the trajectory each time propagation stops and are based on the elapsed time and average geometry of the leg.

## 2. Interplanetary Tracking Dispersions

At the beginning of the scenario for each set of ELEET input parameters, the target ground state is used to initialize a back-propagation to the time of interest, in this case the appointed time for ETM execution. At this point, errors are applied to the position and velocity state of the ERO, sampled according to normal distributions defined by expected knowledge errors vs. time from entry for the Deep Space Network (DSN) and European Space Tracking (ESTRACK) network. This error sampling constitutes the moment when a single nominal state is expanded to a Monte Carlo population of N iterations that will be handled in parallel. Typically, N is set to ten thousand iterations, but can easily be tuned down for speed or up for higher statistical significance.

A similar effect is applied again between maneuvers, when ground tracking would occur to improve the knowledge solution of the spacecraft to plan for maneuvering. The subsequent maneuver is designed according to this solution, which is made imperfect through the addition of position and velocity uncertainties as a function of distance from Earth and time available for tracking/planning. After the initial expansion to N individual iterations pre-ETM, each gets its own randomly-sampled errors and maneuver designs at each stopping point; no further expansion takes place.

## 3. Maneuver Targeting

At the appointed time of ETM execution, ELEET solves for the required maneuver that the ERO must execute to land at the target latitude and longitude aimpoint. Likewise for the FCM, but this maneuver is nominally zero and exists to clean up the ETM execution errors. In some parameter sets, the FCM is deactivated, in which case ELEET foregoes all this computation. This key exploration will be detailed in [section IV](#) as it led directly to conclusions recommending the inclusion of an FCM due to its strong influence on EES delivery accuracy. Solving for an ETM requires that ELEET’s targeter function be seeded with an initial maneuver guess to hit near the target, or the solver will fail when the trajectory fails to intersect with Earth.

The targeting routine is comprised of a locally-linearized two-dimensional Newton-Raphson solver with an iteration limit. All N Monte Carlo samples are processed in a single call, solving a specific maneuver for each sample, but the iteration continues until all points in the batch are within the specified tolerance or until the limit has been reached.

For each sample, an initial error is determined by propagating the initial guess to the atmosphere and then through the atmospheric database (subsection 6) to a landing latitude/longitude coordinate; this coordinate is compared to the input target to determine an initial error. The targeter then tests the sensitivity of the system by adding a small velocity (V) and binormal (B) maneuver component and propagating to find a seed matrix of partial derivatives. The linear system is inverted to find the required maneuver for each individual sample and iterated. Because the Earth is round and the atmosphere behaves stochastically, the system is not truly linear and so the targeter is allowed to iterate a few times, within a limit to prevent infinite loops due to “tolerance ping-pong”. Typically, the tolerance of 0.01 deg of latitude and longitude are converged for the entire set in 2-3 iterations; a limit of 5 iterations is imposed. A  $\Delta V$  perturbation is 0.5 m/s in each V and B directions to seed the solver.

In reality, the maneuver would be allowed to include a third dimension (normal, N) component, but it has been omitted here for simplicity. Once converged, everything is converted back from VNB to Cartesian space and passed back to the main ELEET function along with a count of rogue cases. Equations 6 and 7 display the primary relation behind the Newton-Raphson targeter, which assumes local linearity and zero off-axis partial derivatives. For the sake of speed, his function is solved for a stack of states at once and iterated until all have achieved convergence.

$$dpos = \frac{dpos}{dV} * d\Delta V \quad (6)$$

$$dpos = \begin{bmatrix} dlat \\ dlon \end{bmatrix}, \frac{dpos}{d\Delta V} = \begin{bmatrix} \frac{dlat}{dN} & \frac{dlat}{dlon} \\ \frac{dlat}{dB} & \frac{dlat}{dB} \end{bmatrix}, d\Delta V = \begin{bmatrix} dN \\ dB \end{bmatrix} \quad (7)$$

Each of the N Monte Carlo iterations receives its own solution for the necessary maneuver to hit the common target. Each of these tailored maneuvers also receives its own set of associated execution errors.

For speed, this targeting is not performed to solve for each EAM, which is instead solved as a one-dimensional pure binormal maneuver that is increased until a sufficient perigee altitude is achieved; overshoot and accuracy are ignored. The maneuver execution error for the EAM is still computed, but it has no effect on the EES landing accuracy because it occurs after release. The magnitude as a function of orbit shape and timing are the primary interesting characteristics of the EAM, feeding directly into the ERO propellant budget FOM. Further work would examine the detailed targeting of this maneuver to ensure long-term quarantine of the ERO after leaving the Earth system, but that is beyond the scope of this investigation.

#### 4. Maneuver Execution Errors

For each maneuver, execution errors are applied to each dispersed state’s nominal  $\Delta V$  solution. ELEET’s maneuver execution model consists of three components, based on the behavior and performance of ESA’s recent ExoMars Trace Gas Orbiter (TGO) spacecraft as a starting guess for ERO. First, an uncertainty proportional to the magnitude of the maneuver applied along the nominal thrust axis, representing an over-/under-burn. Second, an uncertainty of fixed magnitude is also applied in the direction of the maneuver. Lastly, a spacecraft pointing (angular) error is generated from a Gaussian input to determine the error between the actual and nominal thrust axes, the azimuth of which is generated from a uniform distribution. These three components combined create an uncertainty “cone” where the resultant  $\Delta V$  could be applied as displayed in Figure 2. The statistical model of each of these three components is dependent upon the nominal  $\Delta V$  of the maneuver, to emulate the difference between spacecraft propulsion systems which would execute it, as displayed in Table 1. For comparison, historical values for proportional error range from 0.5% to 6%, 1 to 40 mm/s in fixed error, and 0.1 to 1.2 deg in angular error.

**Table 1. ELEET Maneuver Execution Error Component’s Statistical Distributions, Based on TGO**

Applicable Maneuver $\Delta V$	$3\sigma$ Proportional Error (%)	$3\sigma$ Fixed Error (mm/s)	$3\sigma$ S/C Pointing Error (deg)
$\Delta V > 0.85$ m/s	0.5	40	0.3
$0.85$ m/s $> \Delta V > 0.15$ m/s		Linearly Interpolated	
$0.15$ m/s $> \Delta V$	2	3	0.6

Commented [AMD1]: Source?

Commented [AMD2R1]: TBD from Kelley/Massimo/Jakob. If not, leave it out and just say its based on ESA past performance.

Commented [AMD3]: Source(s)?

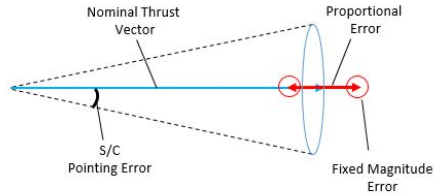


**Figure 2. An illustration of the three independent components of the maneuver execution model implanted in ELEET for ETM and FCM**

In the MATLAB implementation, the maneuver error solver function ingests an  $N \times 3$  array of  $\Delta V$  components where  $N$  is the number of dispersed states in the Monte Carlo, and each of the columns are the X, Y, and Z components of the maneuver's  $\Delta V$ , respectively. By utilizing MATLAB's matrix operations, the corresponding proportional and fixed error for each  $\Delta V$  is randomly sampled from the statistical uncertainty model and applied to every instance of the Monte Carlo simultaneously. To apply the pointing error, a maneuver cone subfunction ingests this dispersed  $\Delta V$  and computes normal and binormal directions relative to each  $\Delta V$  to create  $N$ -many VNB coordinate systems. Within this function, a unit vector is randomly generated from the uncertainty cone given from the statistical distribution of angular error associated with each  $\Delta V$ . Then, each respective  $\Delta V$  is applied along that dispersed direction and then transformed into the EME2000 frame to produce an  $N \times 3$  array of dispersed maneuvers. This is the final dispersed maneuver added to the pre-maneuver velocity state which is then propagated forward to the next node in the EDP. The same general method is also employed in the EES separation mechanism uncertainty model, discussed in the next section.

#### 5. EES Release Error

At the moment of EES release there are two major contributors to the uncertainty in release velocity; the EES release mechanism's performance and the ERO spacecraft's attitude uncertainty. In ELEET, this manifests itself in three numerical uncertainties; the uncertainty in the release mechanism's axial velocity and angular uncertainty, as well as the ERO spacecraft's pointing uncertainty. Table 2 shows the range of uncertainties parametrized in ELEET compared to historical actuals (Stardust, Genesis, Huygens) [7] [8] [9]. At this level of fidelity, any alignment errors or stiffness uncertainties are included in this allocation. It is assumed that the incoming trajectory would be planned such that the final velocity of the EES after release will target the proposed landing site, therefore the nominal  $\Delta V$  from release is biased out in the ELEET nominal trajectory and only the error distribution is considered in this analysis.

The release "maneuver" is applied along the velocity vector as it will be at time of entry to produce an entry angle-of-attack of 0 deg. Similar to the maneuver model, the release error function ingests an  $N \times 6$  array of dispersed position and velocity states at the moment immediately before release, as well as a structure of supporting information including and the entry velocity vector and distribution settings. Once this operation is complete, ELEET propagates the EES to atmospheric interface before activating the entry model.

**Table 2. ELEET EES Release Uncertainty Parameter Ranges and Historical Values**

Model	ELEET Range	Historical Range
$3\sigma$ Axial Velocity Error [mm/s]	0 - 40	9 - 30
$3\sigma$ Separation Mechanism Angular Error [deg]	0 - 5	0.7 - 10
ERO Pointing Error [deg]	0.3	3

#### 6. Atmospheric Entry Model

An important component of ELEET is the atmospheric entry, descent, and landing (EDL) trajectory model. Rather than integrate the full equations of motion for an EDL trajectory for each propagated state in an ELEET analysis, a surrogate EDL model was developed based on a running parametric set of EDL trajectory Monte Carlo analyses. This was done separately to create an EDL database for interpolation. This method offered modest sacrifices to accuracy in exchange for some preparatory work and orders of magnitude decrease in computation time.

This database was parameterized based on three independent variables: the entry flight path angle (EFPA), the entry velocity, and the entry azimuth. For each combination of these variables, a Monte Carlo trajectory analysis was

run with input dispersions on the atmosphere (both density profiles and wind profiles) and the aerodynamics of a representative EES. From each Monte Carlo analysis, key metrics were captured and summarized in an EDL database read by ELEET. For this paper, only landing ellipse size is discussed as a key EDL FOM.

In the present analysis, the EDL database was generated using JPL’s Dynamics Simulator for Entry, Descent and Surface landing (DSEENDS) tool [10]. This multibody physics model is capable of integrating the 6 degree-of-freedom (DOF) equations of motion (although 3-DOF analysis was performed in the current work), and is frequently used to support JPL planetary mission trajectory analysis at Mars and other locations. For ELEET’s purposes, EarthGRAM 2016 was used to create a dispersed set of possible atmospheres at the assumed UTTR landing location at the rough expected entry epoch [11].

The nominal EES aerodynamics were assessed using NASA’s Configuration-Based Aerodynamics (CBAERO) tool for supersonic/hypersonic conditions, and via a curve fit to subsonic test data of 60-deg sphere-cone geometries for transonic and subsonic conditions [12]. The nominal aerodynamic tables were modified during the Monte Carlo analyses via stochastic multipliers on the nominal aerodynamic coefficients. Comparisons were made with higher-fidelity 6-DOF analysis performed by NASA Langley using the Program to Optimize Simulated Trajectories (POST) tool to ensure that the input dispersions and EDL trajectory results used to create the database were consistent with analyses being conducted as part of separate EES formulation work.

The final leg of the ELEET trajectory simulation involves sampling and interpolation of the EDL database in the three inputs parameters for each of the dispersed states at the atmospheric entry. ELEET employs a single function to handle the frame conversions, EDL interpolation, and statistical description of each stack of N entry states, accounting for such effects as expected down/cross-range travel and Earth’s rotation. This yields EDL data as well as landing points which are fit to a multivariate normal distribution to determine the ultimate landing ellipse major axis size. Point cases were used for spot-check V&V against full DSEENDS runs until the database’s accuracy was adequate. ELEET neglects the local topography of the landing area, but it does not neglect local curvature or time-of-flight differences in the atmospheric segment, after it was found that both have noticeable impact on the output.

Performing these operations upon a matrix of dispersed entry states, we can calculate tens of thousands of landing points in a matter of milliseconds due to the N-stack architecture of ELEET, leaving the engineers’ time free to examine a broad tradespace of initial conditions defining each “case”.

### 7. Output Normality Evaluation

It is convenient to describe the landing distribution in terms of Gaussian standard deviations (sigma) for evaluation as the key landing accuracy FOM. While the normality of the output ground ellipse varies from case to case, it was found that the majority of cases do indeed conform to a bivariate normal distribution. This is evaluated in ELEET via the Henze-Zirkler Multivariate Normality Test as implemented by Trujillo-Ortiz, et al (Figure 3) [13] [14].

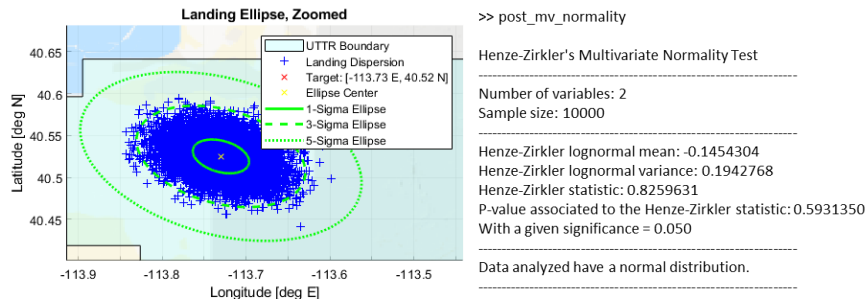


**Figure 3. The Henze-Zirkler Multivariate Normality Test is used in ELEET to determine how appropriate it is to use Gaussian standard deviations to describe the output distribution.**

### 8. End-to-End V&V and Calibration

Near the end of ELEET’s development, additional effort was made to validate the output against the high-accuracy tools used by JPL for navigation of flight missions based on internal python code (MONTE). This method involves a more human-involved design process wherein the navigation team applies a MONTE-based method to sample state covariances and provide that information to the EDL team as a Distributed States File (DSF). This is the mode of

operation of flight entry scenarios like Curiosity and most recently InSight. Point cases were run in ELEET and in the MONTE method and used to identify areas of method improvement. The final form of ELEET was put into use only once the percent-error values between tools was driven down to consistently <10%, instilling confidence good enough for trend exploration. Periodically, when a particular region of the tradespace looks interesting, we delve deeper by examining the point-case in MONTE, and any discrepancies found are used to continually improve ELEET's approximations.

### C. Figures of Merit

The outputs of ELEET include several key FOMs which can be used to inform future trades or decisions. These quantities affect various mission partners and their elements/systems that comprise the EDP. In this section, we'll briefly introduce these FOMs and then the following sections will discuss some interesting trends in the results as pertaining to these FOMs. The impact and decision rationale behind acting on such results is outside the scope of this discussion. They are presented in no ranked order.

#### 1. EES Free-Flight Time

As the EES flies through space without the protection of the ERO and associated hangar, it incurs risk of being struck by micrometeoroid and orbital debris (MMOD), evaluated as an integrated chance of damage over the flight path according to a size fluence distribution. Such damage has the potential to endanger mission success, and so therefore, it is highly desirable to minimize the free-flight time of the EES between release and atmospheric entry, when the EES is outside of its protective hangar.

#### 2. ERO Time on Intercept

To minimize the risk of impacting Earth with the ERO, it is desirable to minimize the amount of time it spends on a trajectory which intersects the surface (or atmosphere) of the planet. Extended time on impact would impose undue expectation on the reliability of the ERO, integrated through time. Preliminary analyses suggest that the ERO would require about one hour to perform a 360-degree flip and settle, so this is used conservatively as a minimum time between events to allow for changes in attitude. That is: EES release is performed no earlier than one hour after the FCM, and the EAM is performed as early as possible, no earlier than one hour after the EES release.

#### 3. Time Margin

Similarly, it is desirable to maximize the time between the nominal release and the last feasible moment to perform EAM, to be allocated as tactical timeline margin. In the event of an off-nominal scenario, this margin would define the amount of time available to be consumed for contingency tracking/planning/SC recovery, for example.

#### 4. ERO Propellant Budget

By virtue of being a SEP sample-return scenario, all propellant mass required to execute the EDP has influence over all previous phases back to launch. ETMs and EAMs performed late (close to Earth) may achieve a higher degree of EES landing accuracy, but would also require additional propellant mass to execute, mass which must be launched and carried throughout the entire ERO mission. The ERO mass ultimately affects the acceleration achievable by the spacecraft, which translates directly to required time for heliocentric SEP orbit transfers. This time is drawn either from margin, or from the ERO surface relay/rendezvous timeline; at a threshold, the timeline will no longer be feasible.

#### 5. Orbital Debris wrt ERO

After EDP, or in the event of an abort scenario, the ERO would have to fly by Earth at a given perigee altitude, subject to conflict with orbital debris in Earth's neighborhood. Orbital debris (OD) can be simply described by a plot of spatial density such as [Figure 4](#) below, via J.-C. [Liou \[12\]](#). Here, one can clearly see that particular altitudes host large concentrations of orbital debris, with spikes corresponding to the 2009 collision of satellites Iridium-33 and Kosmos-2251 and the 2007 Fengyun-1C anti-satellite missile test. Any hyperbolic trajectory would have to pass through all altitudes higher than its perigee twice, and so avoiding these areas of high density is desirable for reducing the risk of damaging the ERO post-EAM as part of long term Earth quarantine.

Further detailed analysis could rigorously quantify OD risk to the ERO, accounting for latitudinal variation and eventually for specific trajectories and specific epochs, but this simple model suffices for ELEET's broad tradespace exploration. For this early analysis, a nominal hyperbolic perigee altitude of 1,600 km was set as a representative target for the incoming and outgoing hyperbolic trajectories. The impacts of varying this parameter on the delivery accuracy and ERO  $\Delta V$  budget were explored, but no attempt was made to quantify the orbital debris risk other than "above/below" the 1,600 km altitude threshold.

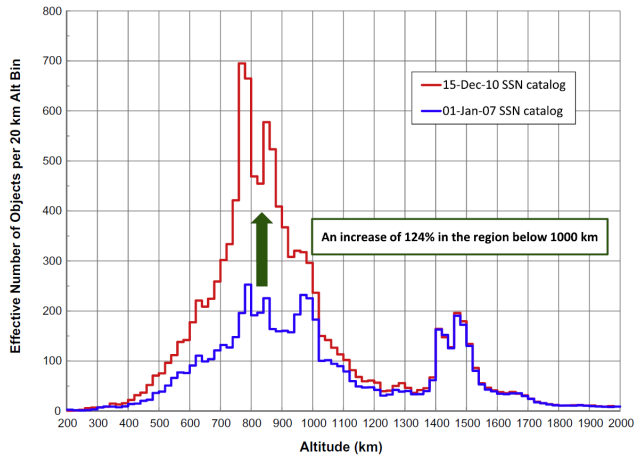


**Figure 4. Liou shows distributions of object count vs. orbit altitude in January 2001 and December 2010 [15]. The large increase in object count during the intervening period can be largely attributed to the Fengyun-1C anti-satellite test and the collision of Iridium-33 and Kosmos-2251.**

#### 6. Landing Ellipse Size and Orientation

The final landing ellipse on the ground is described in ELEET with bivariate 1-, 3-, and 5- $\sigma$  ellipse major/minor axis lengths (km) and azimuthal rotation (in degrees). Recall that bivariate standard deviations are not at the same thresholds as their 1-dimensional analogs. For reference:  $1\sigma = 39.3\%$ ,  $3\sigma = 98.9\%$ ,  $5\sigma = 99.9996\%$ .

Subsequent detailed map analyses could yield an ellipse-placement FOM, but this is future work and not in the scope of the ELEET exploration. The landing accuracy fitness of a given ellipse is described by the extent of its 5- $\sigma$  boundary and taken as an output FOM. Below, [Figure 5](#) shows a representative ellipse on the ground, with UTTR shown for scale.

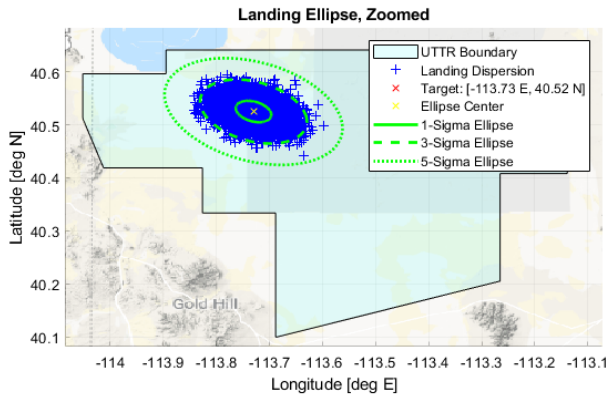


**Figure 5. A representative landing ellipse plotted over the notional UTTR landing site.**

Along-track accuracy (ellipse major axis) and azimuth are largely determined by maneuver accuracy and heliocentric approach respectively, while the minor axis of the ellipse is dominated by the atmospheric flight portion of the trajectory.

## IV. Results

The primary purpose of ELEET is to examine the broad EDP tradespace at a sufficient level of detail to inform high-level trades and decisions in Phase A formulation in a flexible and swift implementation. This section discusses some of the trend observations made throughout this investigation, some expected but others challenging initial intuition.

### A. Select Trends

Perhaps the single most impactful finding of the ELEET investigation is summarized in Figure 6. This plot shows the trend of landing ellipse major axis ( $3\sigma$ ) vs. the timing of EES release with respect to entry interface for the cases of the four permutations of Earth avoidance altitude and inclusion of the optional FCM. We can see here several things, given the other settings and dimensions of this tradespace held constant:

1. Fully satisfying the avoidance altitude constraint without an FCM is not feasible.
2. The inclusion of an FCM effectively nullifies the accuracy effects of difference in avoidance altitude.
3. The inclusion of an FCM drastically improves the landed accuracy performance across the board.
4. The FCM curves allow for some trade to be made between landed accuracy fitness and timeline margin.
5. There are feasible, even close-to-ideal, solutions to this problem.

This trend can be explained through simple logic, evident ex post facto: higher avoidance altitudes require a larger ETM to target the nominal aimpoint, which leads to larger proportional maneuver errors. Unchecked (without an FCM), these effects lead to very large landing ellipses. The FCM helps to nullify this error (“clean it up”), but the small remaining errors are amplified over time for early releases, so accuracy improves as release waits. Later maneuvers have larger magnitudes as well and therefore larger errors, but less time to propagate, so there is an inflection in the trend but not a saddle point.

An old design point (circa 2003-2005) is shown as the red dot, the major difference being that a much larger ellipse size was tolerable for that design for many reasons including reduced range risk and the possibility of a parachute soft-landing, opening up a larger feasible landing area. The impact of this more stringent accuracy goal was originally discounted, and magnitude of the benefit afforded by including an FCM was a surprising finding. Avoiding extraneous maneuvers is another approach to risk reduction, but foregoing FCM was not found to be feasible in this tradespace.

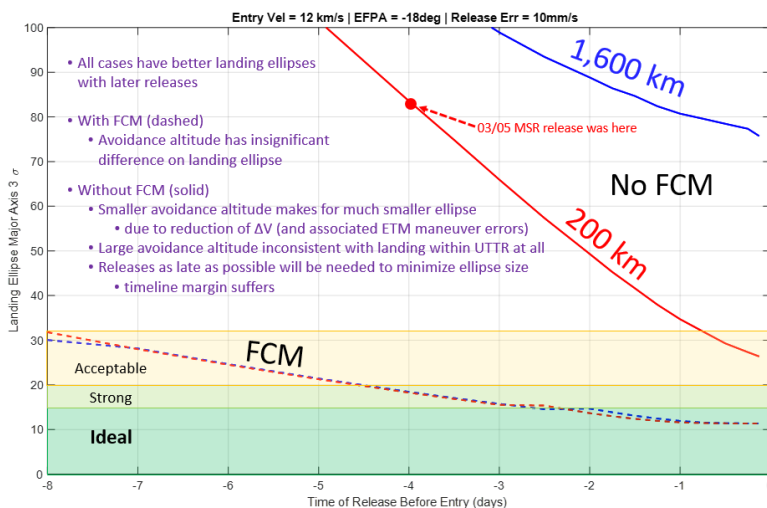


Figure 6. A driving trend discovered during the ELEET investigation was the impact of maneuver execution errors on the final landed accuracy, and how that was affected by the inclusion of an FCM.

Figure 7 shows how another key trend: how the landed accuracy of three different EFPA cases trend with release timing and axial release velocity. For example: for an EFPA of -25 deg (green dot-dash), if a 20-km landing ellipse is to be maintained while changing the axial release error from 10 to 30 mm/s, the release time would have to slide from -6 to -2.5 days. Alternatively, for a given release timing and ellipse size, a steeper EFPA can tolerate a higher degree of release velocity uncertainty.

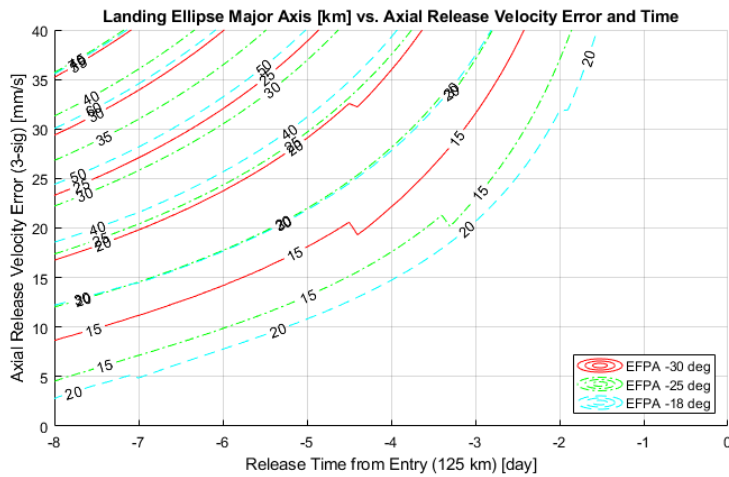


Figure 7. These three contours show how landed accuracy trends with release timing and axial release velocity error for three example EFPA values. Note the kink in the contour, a quantization error.

From this plot, we can glean several important lessons, some more obvious than others:

1. Decreasing the time from release to entry decreases landing ellipse size for a given EFPA.
2. Increasing the release velocity error increases landing ellipse size for a given EFPA, this trend becomes less apparent for later ellipses.
3. For a given case of entry timing and release velocity error performance, steeper EFPAs offer tighter landing ellipse sizes.

The hyper-dimensional output of an ELEET tradespace allows us to make special plots to compare any number of quantities whenever a new, unique question arises, and this plot is an example of one of those bespoke analyses.

These two figures suggest minimizing time from release to entry and making the EFPA as steep as possible, while trying to keep release mechanism errors low. An example of an opposing FOM is shown in Figure 8. Here we can see a strong relationship between release timing and the total maneuver magnitude required for the EDP scenario. One can also note a weak relationship between EFPA and maneuver budget. From this we clearly glean one major conclusion resistive to the prior: the ERO suffers from late release at exponential rate. Recall that this FOM affects the mass of the ERO, which affects the overall mission timeline feasibility. Additionally, recall the resistive FOM of EDP timeline margin, whose impact is less quantifiable.

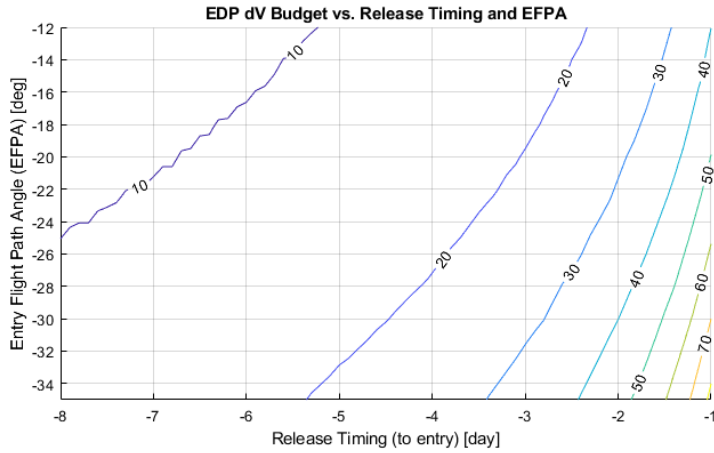


**Figure 8.** This contour map shows how the EDP maneuver budget trends as a function of EFPA and release timing. This map shows a strong relationship in one dimension and a weak relationship in another.

### B. Scenario Behaviors

In addition to trends across the tradespace, ELEET helped us understand the general character of the problem and how the solution behaved. See below [Figures 9 and 10](#), histogram fits of the resultant EFPA, entry timing, and resultant maneuver magnitudes. The output entry state represents a convolution of all the upstream effects, so the shape of the output distribution was a question during formulation. One can readily see that each quantity behaves in a manner that can be described with Gaussian standard deviations and compared to historical analyses, requirements, and actuals.

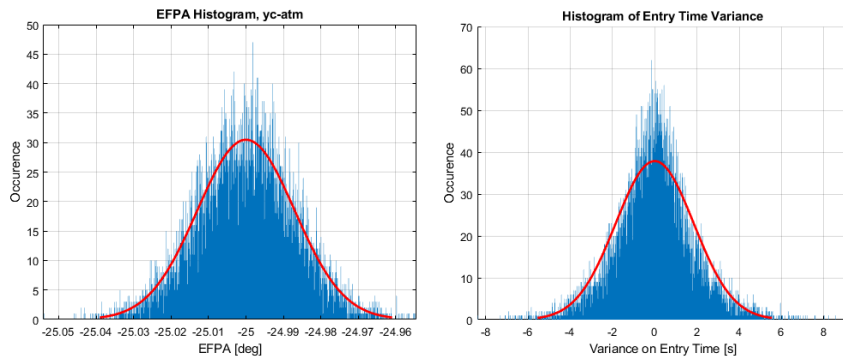


**Figure 9.** Statistical distribution of EFPA (left) and entry timing (right) for all N iterations of a given case. Most cases were found to be well-behaved and easily approximated by Gaussian statistics, as well as in-family with heritage examples such as Stardust ( $-0.08$  deg corridor) and Genesis.

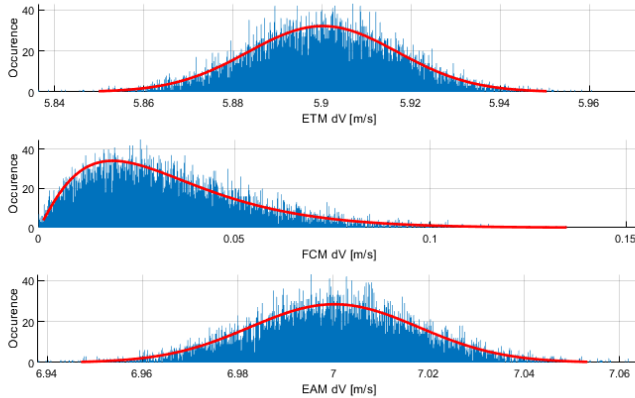


**Figure 10.** Statistical distribution of maneuver magnitudes for each maneuver of a representative case EDP scenario. Again, ETM and EAM well behaved about a nominal value. FCM interestingly has a left-skew with the expected value not at zero, due to the fixed in-line maneuver error incurred whenever FCM is included in the sequence.

## V. Conclusions

The single most driving tradeoff was found in the timing of the beginning (ETM) and end (EAM) of the EDP sequence with relation to the landed accuracy. The timing of the sequence directly drives the size of the maneuvers, which then drives the proportional error distributions on those maneuvers, but is overtaken by astrodynamics, so one sees a diminishing return. It was found that including the optional FCM served to greatly increase the delivered accuracy, enabling access to a large portion of the tradespace that would otherwise be invalid, mostly due to poor landed accuracy. Extending the time between ETM and FCM would allow for a reduction of ETM magnitude without sacrifice to landed accuracy, but at the cost of increased time-on-impact and reduced time margin, other key FOMs.

Along-track landing ellipse error (major axis) was found to be dominated by maneuver execution error and exacerbated by shallow EFPA values, while the landing ellipse cross-track (minor axis) size was found to be dominated by atmospheric effects. Landing accuracy and the ERO's propellant budget are almost directly at odds, along with EDP timeline margin.

No inputs or output FOMs were found to be of negligible consequence, but maneuver error was found to be the dominant factor (without an FCM). When mitigated with an FCM, the EES release errors and atmospheric effects were found to be on comparable order and traded dominance as a function of EDP timing. The target geometry (EFPA, nominal miss altitude) had a moderate impact, and navigation accuracy's effect was minimal.

With the exception of very shallow EFPA cases, results were found to be well-behaved, producing smooth trends and often lending well to Gaussian fits. The exception shallow cases tended to be very sensitive to input conditions and error distributions (e.g. failing to hit Earth due to ETM errors) and so ELEET's approximations were not valid for this regime. This had little consequence, since steeper EFPA values were found to offer favorable landing accuracy.

The investment of effort that went in to producing the ELEET tool paid off in communicating the balance of EDP resources (e.g. time,  $\Delta V$ , accuracy) between sub-phases and mission elements in the program, allowing teams to work to defined boundaries early in formulation. ELEET continues to serve as a valuable systems engineering tool to examine the exchange rate of EDP resources between elements as current-best-estimates of quantities evolve. The authors intend to carry on the philosophy of examining the entire problem, and its surrounding region, to identify lurking threats and hidden opportunities amongst hyper-dimensional tradespaces.

### Acknowledgments

The authors acknowledge that this effort has been a small part of the great team undertaking that is MSR and would like to thank everyone involved in the development of ELEET, particularly Robert Haw, Scott Perino, James Corliss, Jeremy Vander Kam, and Robert Lock. They also acknowledge the parallel work and inputs from the MSR and ERO teams in Europe.

The information presented about potential Mars sample return architectures is provided for planning and discussion purposes only. NASA has made no official decision to implement Mars Sample Return. This work was carried out at the Jet Propulsion Laboratory, California Institute of Technology, under contract to NASA. Government sponsorship acknowledged.

### References

- [1] B. K. Muirhead, A. K. Nicholas, J. Umland, O. Sutherland and S. Vijendran, "mars Sample Return Mission Concept Statu," in *70th Interantional Astronautical Congress*, Washington, DC, 2019.
- [2] R. E. Lock, A. K. Nicholas, S. Vijendran, R. C. Woolley, A. M. Didion, F. Laipert and Z. Olikara, "Potential Campaign Architectures and Mission Design Challenges for Near-Term International Mars Sample Return Mission Concepts," in *AAS/AIAA Space Flight mechanics Meeting*, Ka'anapali, HI, 2019.
- [3] A. K. Nicholas, A. M. Didion, F. Laipert, Z. Olikara, R. C. Woolley, R. E. Lock and J. Huesing, "Mission Analysis for a Potential Mars Sample Return Campaign in the 2020's," in *AAS/AIAA Space Flight Mechanics Meeting*, Ka'anapali, HI, 2019.
- [4] M. Lobbia, S. Perino, J. Vander Kam and J. Corliss, "Robotic Mars Sample Return and Earth Entry Vehicle Concept Development," in *32nd ISTS & 9th NSAT*, Fukui, Japan, 2019.
- [5] O. Sutherland, S. Vijendran, J. Huesing, K. Geelen, D. Feili, J. M. Sanchez-Perez, A. Nicholas and R. Lock, "Mars Sample Return - Earth Return Orbiter: ESA's next Interplanetary Electric Propulsion Mission Concept," in *36th International Electric Propulsion Conference*, Vienna, Austria, 2019.
- [6] D. A. Vallado, *Fundamentals of Astrodynamics and Applications*, Second Edition, Springer, 2007, pp. 90-103.
- [7] P. N. Desai and F. M. Cheatwood, "Entry Dispersion Analysis for the Genesis Sample Return Capsule," *Journal of Spacecraft and Rockets*, vol. 38, no. 3, pp. 345-350, 2001.
- [8] P. N. Desai, D. T. Lyons, J. Tooley and J. Kangas, "Entry, Descent, and Landing Operations Analysis for the Stardust Re-Entry Capsule," in *AIAA/AAS Astrodynamics Specialist Conference and Exhibit*, Keystone, CO, 2006.
- [9] U. R. Herlach, P. Tatalias, B. Schmid and D. Mussett, "Huygens Separation Mechanisms," in *Sixth European Space Mechanisms & Tribology Symposium*, Zurich, Switzerland, 1995.
- [10] J. Balam, R. Austin, P. Banerjee, T. Bentley, D. Henriquez, B. Martin, E. McMahon and G. Sohl, *DSEND5 - A High-Fidelity Dynamics and Spacecraft Simulator for Entry, Descent, and Landing*, IEEE Paper AC-302, 2001.
- [11] F. W. Leslie and C. G. Justus, "The NASA Marshall Space Flight Center Earth Global Reference Atmospheric Model- 2010 Version," NASA Marshall Space Flight Center, Huntsville, AL, 2011.
- [12] D. J. Kinney, "Aero-Thermodynamics for Conceptual Design," in *42nd AIAA Aerospace Sciences Meeting and Exhibit*, Reno, NV, 2004.
- [13] N. Henze and B. Zirkler, "A class of invariant consistent tests for multivariate normality," *Communications in Statistics- Theory and Methods*, vol. 19, no. 10, pp. 3595-3617, 1990.
- [14] A. Trujillo-Ortiz, R. Hernandez-Walls, K. Barba-Rojo and L. Cupul-Magana, "HZmvntest: Henze-Zirkler's Multi-variate Normality Test. A MATLAB file.," 12 2007. [Online]. Available: <https://www.mathworks.com/matlabcentral/fileexchange/17931-hzmvntest>. [Accessed 1 2019].
- [15] J.-C. Liou, "An active debris removal parametric study for LEO environment remediation," *Advances in Space Research*, vol. 47, pp. 1865-1876, 2011.